# Journal Pre-proof

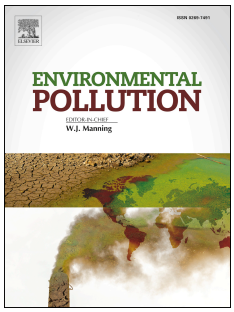


Treatment of microplastics in water by anodic oxidation: a case study for polystyrene

Marthe Kiendrebeogo, M.R. Karimi Estahbanati, Ali Khosravanipour Mostafazadeh, Patrick Drogui, R.D. Tyagi

PII: S0269-7491(20)36857-3

DOI: https://doi.org/10.1016/j.envpol.2020.116168

Reference: ENPO 116168

To appear in: *Environmental Pollution*

Received Date: 16 July 2020

Revised Date: 23 November 2020

Accepted Date: 25 November 2020

Please cite this article as: Kiendrebeogo, M., Estahbanati, M.R.K., Mostafazadeh, A.K., Drogui, P., Tyagi, R., Treatment of microplastics in water by anodic oxidation: a case study for polystyrene, *Environmental Pollution*, https://doi.org/10.1016/j.envpol.2020.116168.

## AUTHORSHIP STATEMENT

**Marthe Kiendrebeogo**: Conceptualization, Methodology, Validation, Investigation, Writing - Original Draft, Visualization.

**M.R. Karimi Estahbanati**: Conceptualization, Methodology, Validation, Investigation, Writing - Original Draft, Writing - Review & Editing, Visualization, Supervision.

**Ali Khosravanipour Mostafazadeh**: Validation, Investigation, Writing - Review & Editing.

**Patrick Drogui**: Conceptualization, Methodology, Validation, Investigation, Resources, Writing - Original Draft, Writing - Review & Editing, Supervision, Project administration, Funding acquisition.

**RD. Tyagi**: Validation, Investigation, Resources, Writing - Review & Editing, Funding acquisition, Project administration.

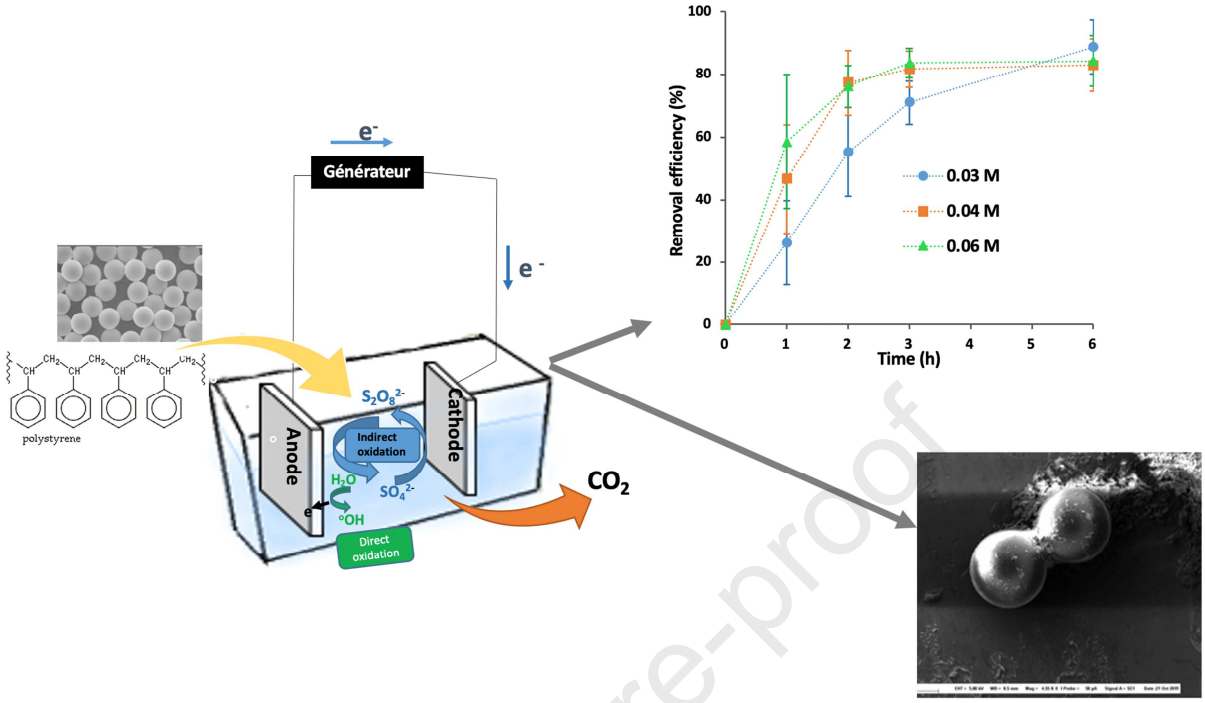

# Treatment of microplastics in water by anodic oxidation: a case study for polystyrene

Marthe Kiendrebeogo[1], M.R. Karimi Estahbanati[1], Ali Khosravanipour Mostafazadeh[1], Patrick Drogui[1*], RD. Tyagi

[1] Institut national de la recherche scientifique (INRS) - Centre Eau Terre Environnement (ETE), 490 rue de la Couronne, Québec (QC), CANADA, G1K 9A9

*Corresponding authors: patrick.drogui@ete.inrs.ca

## Abstract

Water pollution by microplastics (MPs) is a contemporary issue which has recently gained lots of attentions. Despite this, very limited studies were conducted on the degradation of MPs. In this paper, we reported the treatment of synthetic mono-dispersed suspension of MPs by using electrooxidation (EO) process. MPs synthetic solution was prepared with distilled water and a commercial polystyrene solution containing a surfactant. In addition to anode material, different operating parameters were investigated such as current intensity, anode surface, electrolyte type, electrolyte concentration, and reaction time. The obtained results revealed that the EO process can degrade 58 ± 21% of MPs in 1 h. Analysis of the operating parameters showed that the current intensity, anode material, electrolyte type, and electrolyte concentration substantially affected the MPs removal efficiency, whereas anode surface area had a negligible effect. In addition, dynamic light scattering analysis was performed to evaluate the size distribution of MPs during the degradation. The combination of dynamic light scattering, scanning electron microscopy, total organic carbon, and Fourier-transform infrared spectroscopy results suggested that the MPs did not break into smaller particles and they degrade directly into gaseous products. This work demonstrated that EO is a promising process for degradation of MPs in water without production of any wastes or by-products.

**Keywords:**

Microplastic; polystyrene; electrooxidation; degradation; polymer.

## 1. Introduction

Plastics are used in all consumer sectors, so that global production is growing every year. It rose from 322 million tons in 2015 to 360 million tons almost in 2018 (Plastics, 2019). It is estimated up to 10% of the produced plastics fragments would be found in the marine environment (Cole et al., 2011). Once present in the marine environment, the plastics undergo aging processes that cause their degradation and fragmentation into small particles called microplastics (MPs, particles less than 5 mm) (Lambert and Wagner, 2016) and then into nanoparticles (particles less than 100-1000 nm)(Gigault et al., 2018). Polystyrene is one of the most widely used commercial plastic in the world (Wegner et al., 2012; Zarfl and Matthies, 2010), therefore, it is one of the most commonly found polymers in marine environments (Hidalgo-Ruz et al., 2012; Moore, 2008).

The release of MP into the marine environment is recognized as an important problem related to water pollution (Lambert and Wagner, 2016). It has been shown that in aquatic environments, these MPs adsorb toxic substances and can be ingested by aquatic organisms. Afterwards, they accumulate in the food chain and subsequently reach humans (Bouwmeester et al., 2015; Chae and An, 2017). Among different toxic effects on aquatic organisms which have been proved by previous studies, there is a decrease in growth rate, fertility, lifespan, and reproductive time (Besseling et al., 2014; Jeong et al., 2016; Wegner et al., 2012). Polystyrene is a plastic material whose toxicity has been widely demonstrated (Besseling et al., 2014; Lee et al., 2013; Rossi et al., 2014).

Although MPs are detected at low concentrations in wastewater treatment plants' effluents, these effluents are still a potential way to release MPs because of the large volume of effluents discharged into the aquatic environment (Ziajahromi et al., 2017). It has been shown that the wastewater treatment plants fragment 80% of MPs into nanoplastics which can increase the number of plastic particles around 10 times (Enfrin et al., 2019). The concentration of MPs with size of 10-300 µm in wastewater treatment plants' influents and effluents has been reported in a range of 1-10044 and 0-447 particles/L, respectively (Sun et al., 2019). Accordingly, the conventional treatment is unable to completely remove the MPs and it is essential to develop other technologies to remove MPs in the effluent of wastewater treatment plants.

The previous efforts to develop such technology focused on the separation processes such as rapid sand filtration, disc filtration, dissolved air flotation, MBR/ultrafiltration, dynamic membrane filtration, and electrocoagulation (Lares et al., 2018; Li et al., 2018; Perren et al., 2018; Talvitie et al., 2017). Since all of these technologies just separate MPs and does not degrade them, additional efforts are required to manage the separated MPs. A limited research concerned the degradation of MPs and most of these works performed on photocatalytic degradation of MPs which showed generally a couple of weeks is required to obtain an acceptable degradation efficiency (Phonsy et al., 2015; Satoshi et al., 1998). This long processing time does not present a bright perspective because of the current photocatalysis technology. Therefore, development of efficient technologies to degrade MPs in a reasonable time scale is essential. In addition, the degradation processes should be studied to evaluate the possibility of developing a hybrid zero-discharge process by coupling (i) the separation of MPs into a concentrated stream with (ii) the degradation of MPs in the concentrated stream. This configuration hinders the discharge of small MPs into the aquatic environments.

In recent years, electrooxidation (EO) process has been developed for the degradation of persistent pollutants, such as pesticides, dyes, pharmaceuticals, and petrochemicals found in effluents (Francisca et al., 2013; Ganiyu et al., 2017; Garcia-Segura et al., 2015; Souza et al., 2015; Yassine et al., 2018; Zhuo et al., 2016). This process is environmentally friendly as it could degrade MPs into nontoxic molecules like water and carbon dioxide without addition of chemicals. EO is based on *in-situ* generation of oxidizing radicals like hydroxyls ($^{\bullet}OH$) by direct and indirect electrochemical process. The standard reduction potential of hydroxyl radicals (E ($^{\bullet}OH$ /$H_2O$): 2.80 V/SHE) allows it to break the polymeric bonds of MP and degrade them. Therefore, EO is a promising zero sludge technology to degrade MPs at atmospheric condition. To the best of our knowledge, there is no work on electrooxidation of MPs found in the literature.

The aim of this study was to explore the degradation of MPs from water using anodic oxidation. As polystyrene MPs exhibit the highest toxicity among common MPs, polystyrene microbeads with 26 µm size were used as a representative MP. An experimental approach was followed to determine the best operating parameters of the EO process (current intensity, anode surface area, anode material, electrolyte type,

electrolyte concentration, and time) to effectively oxidize MPs in water. For each parameter, the MPs degradation performance was evaluated using removal efficiency and mode size of MPs, which were obtained by weight loss and dynamic light scattering (DLS) analyses, respectively. The samples were examined by microscopic, spectroscopic, and total organic carbon (TOC) analyses to evaluate the shape and size, surface functional groups, and formed by-products, respectively, and then evaluate the obtained results through parametric study. In addition, total current efficiency of the EO process was evaluated and an economic analysis was conducted for different conditions. Finally, a mechanism of polystyrene degradation was proposed based on the obtained results.

## 2. Materials and methods

### 2.1. Preparation of water sample

The mono-dispersed suspension of polystyrene microbeads with 10% MP concentration (100 g/L) supplied by thermo scientific USA and used as the MP source. The nominal diameter and uniformity of size of MPs were 25 μm and 15%, respectively. These microbeads were used to make 100 mg/L MP suspension in deionized water. The suspensions were prepared spontaneously before starting the experiments. The amount of added electrolyte for the improvement of electrical conductivity was 4.25, for both $Na_2SO_4$ and $NaNO_3$, and 3.50 g/L for NaCl. These amounts correspond to 0.03, 0.05, and 0.06 M, respectively. The pH of all prepared solutions was approximately 6.0. Finally, 50 mL samples were taken to characterize the sample before treatment.

### 2.2. Experimental unit

The EO reactor was made of plexiglass with dimensions of 14.5 × 6.4 × 17.7 cm and an operating volume of 900 mL. All experiments were made in batch mode. Boron-doped diamond (BDD), mixed metal oxide (MMO), and iridium oxide ($IrO_2$) electrodes were employed as anodes and titanium electrode was used as cathode. The electrodes were gridded and had a circular shape with a diameter of 12 cm, a thickness of 0.1 cm, and a surface area of 113.1 $cm^2$. In the reactor, the anode and cathode were fixed vertically with 1 cm space and were connected to the positive and negative outputs of a DC power

supply, respectively. The reactor was placed in a box containing ice cubes to put the entire external surface of the reactor in direct contact with the ice cubes.

### 2.3. Experimental procedure

The tests were carried out at room temperature. The temperature of solutions was followed by a scientific J-KEM thermocouple. To mitigate the evaporation of solution due to the temperature rise caused by electrooxidation at high current intensities, a cooling system was employed. The solution was mixed by agitation with a magnetized bar. In a typical experiment, the current densities set at 108 and 216 $mA.cm^{-2}$ for BDD, 108 $mA.cm^{-2}$ for MMO, and 433 $mA.cm^{-2}$ for $IrO_2$. In addition, the initial concentration of microbeads and the electrolyte concentration ($Na_2SO_4$) were set at 100 mg/L, and 0.03 M, respectively. The sampling time was 1, 2, 3, and 6 h. To assure that high water temperature (which was observed in a few experiments at high current) has no effect on the results, a control test carried out without electrooxidation at 100°C for 6 h. EO tests consisted of analyzing different operating parameters, such as current density (3, 6, and 9 A), types of oxygen-intensive anodes (BDD, MMO, and $IrO_2$), anode surface area (41.5 and 83 $cm^2$), and type ($Na_2SO_4$, $NaNO_3$, NaCl) as well as concentration (0.03, 0.04, 0.06 M) of electrolyte.

### 2.4. Analytical procedure

The electrooxidation of MPs performance was assessed by combining the evolution of the particle size profile of MPs with the mass loss of MPs over time. In addition, scanning electron microscopy (SEM), Fourier-transform infrared spectroscopy (FTIR), and TOC analyses were performed to evaluate the obtained results.

#### 2.4.1. Particle size analysis

The particle size distribution of MP in water was measured by dynamic diffusion of light using a particle size analyzer (Laser Scattering Particle Size Distribution Analyzer LA-950, HORIBA, 0.01-3000 µm). A refraction index of 1.59 was used for the analyses. In addition to particle size distribution, the mode size distribution was considered for assessment of the particle size during treatment. For each analysis, 50 ml of sample was injected into the particle size analyzer.

### 2.4.2. Removal efficiency analysis

The elimination of MPs was followed by measuring the weight of MPs in 50 ml samples taken during the EO treatment. The samples were filtered with 0.22 µm pore size nitrocellulose filters to separate the MPs. The filters were then dried in an oven at 40 °C for 24 hours to evaporate water. The amount of remained electrolyte salt in the filter after drying was measured using electrolyte solutions without MP. These data were used to correct the errors due to the remaining salt in the filters during the analysis of MP degradation. The mass loss of MP was calculated using Eq. (1):

$$\text{Weight loss } (\%) = \frac{W_0 - W_t}{W_0} \times 100 \quad (1)$$

where $W_0$ and $W_t$ are the initial and final mass of MPs, respectively.

In order to calculate the total current efficiency (TCE) for anodic oxidation of MP, the COD values of the water before and after treatment were determined by MA. 315–DCO 1.1 method. The samples were first digested in a CR 3200 thermo reactor at 150°C for 2 h. The COD values were then obtained by analysis of the samples using Spectrophotometer-Vis UV0811M136. The TCE values were then calculated using the following equation (Ciríaco et al., 2009; Durán et al., 2018):

$$TCE\ (\%) = FV_s \cdot \frac{(COD_0 - COD_t)}{8I\Delta t} \times 100 \quad (2)$$

where $COD_0$ and $COD_t$ are initial and final chemical oxygen demands, respectively, in g $O_2$. $L^{-1}$, I represents the current intensity (A), F is the Faraday constant (96487 C $mol^{-1}$), $V_s$ is the water volume (L), 8 is the oxygen equivalent mass (g $eq.^{-1}$), and Δt is the electrooxidation time interval (s).

### 2.4.3. SEM analysis

The size and shape of MPs before and after EO were analyzed by SEM analysis. After mixing, 1 mL of sample was placed on specimen stub and dried at room temperature for 24 hours. The samples were then covered with a layer of gold by SPI coasting device to make them electrically conductive. The shape and size of MPs were analyzed using ZEISS EVO 50 smart device. The INCA software was used to capture the images.

### 2.4.4. FTIR analysis

For FTIR analysis, 700 mL of sample was filtered to separate the MPs. The MPs were then analyzed by FTIR Spectrometer (Nicolet 50, Thermo Fisher, USA) equipped with an

attenuated total reflectance (ATR) diamond crystal module. The range of scanning set from 500 to 4000 $cm^{-1}$ and the collection time was 16 s. The obtained spectrums were compared with the reference spectrum recorded with particles before EO.

### 2.4.5. TOC analysis

The presence of dissolved organic carbon in the samples during the EO was analyzed after filtration of remained MPs through a filter with pore size of 0.22 µm to evaluate the generation of by-products. Nitrocellulose filter was used for separation of the remained MPs. The TOC analysis was then conducted using Shimadzu VCPH device.

## 2.5. Economic analysis

To conduct the economic analysis, the energy consumption was first calculated using Eq. (3):

$$Energie\ consumption\ \left(KWh/_{m^3}\right) = \frac{I \times T \times t}{V} \times 10^{-3} \quad (3)$$

where I, T, t, and V represent current intensity (A), electrical potential (v), time (h), and volume ($m^3$), respectively. Energy consumption and electrolyte costs were two factors considered for estimating the operating cost of EO. The cost of electricity was estimated based on a unit cost of 0.3, 0.06, 0.4 $US/kg for $Na_2SO_4$, NaCl, and $NaNO_3$, respectively.

# 3. Results and discussion

## 3.1. Characterization of MPs

Figure 1a depicts the size distribution of MPs before EO which obtained by DLS analysis. It was observed that the size range is 17-45 µm and the distribution is unimodal with 26 µm mode size with a standard deviation of 4 µm. The mode size is close to the nominal diameter size of 25 µm which indicated by the supplier. The respective D10, D50, and D90 were obtained at 21.20, 26.15, and 32.60 µm, respectively. Figure 1b shows the morphology of particles which obtained by an optical microscope. It can be seen that all the particles are in spherical shape that confirms the obtained values from DLS analysis were the diameter of spheres.

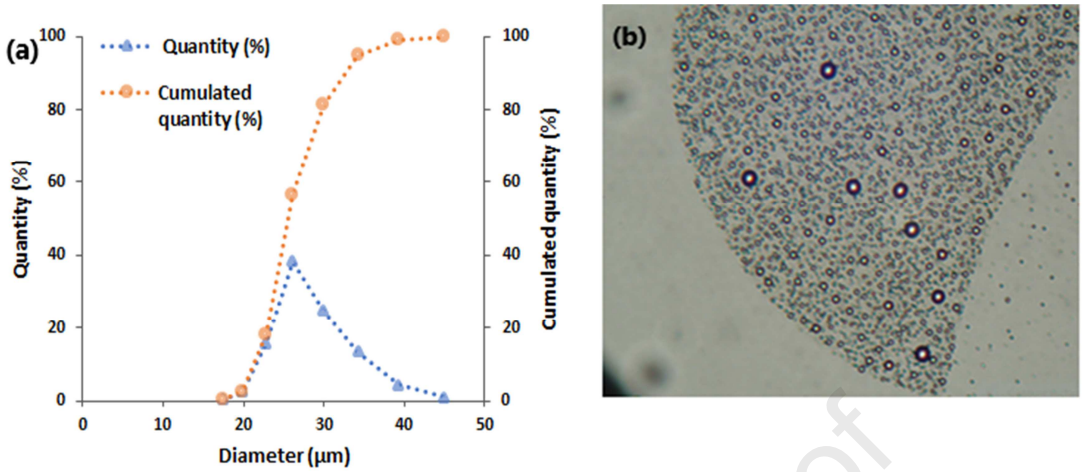


**Figure 1.** (a) Size distribution of the used MP, (b) a view of MPs under an optical microscope.

205

206 **3.2. Parametric study of MPs EO**

207 **3.2.1. Effect of the applied current intensity**

208 In order to investigate the effect of current intensity, a series of experiments were
209 conducted at 3, 6, and 9 A using BDD and 0.03 M $Na_2SO_4$ solution. Figure 2 depicts
210 mass removal percentage and MPs mode size over EO time. It shows a significant effect
211 of current intensity on the MPs weight loss and a reduction in the MPs size. It can be seen
212 that the weight loss starts from the beginning of treatment and increases depending on the
213 current intensity. To achieve an elimination efficiency of 89 ± 8%, an EO operating time
214 of 6 hours was required with a current intensity of 9 A (which is equal to the current
215 density of 108.4 $mA.cm^{-2}$). A degradation efficiency of 56 ± 10% was recorded at 6 A
216 (72.28 $mA.cm^{-2}$) and a very low degradation of MP was observed at 3 A (36.14 $mA.cm^{-2}$).
217 A very good degradation efficiency at 9 A could be explained by the high sensitivity
218 of BDD to the current intensity. The higher applied current density allowed the anode to
219 oxidize more water molecules into hydroxyl radicals that helps in the enhancement of
220 MPs oxidation. To compare with previous studies, for washing machine effluent
221 treatment which contained microfibers, a COD removal of 85% was achieved at 180 min,
222 current density of 66.6 $mA.cm^{-2}$, and $Na_2SO_4$ concentration of 7 g/L (Durán et al., 2018).
223 In order to analyze the size of MPs during the EO process, the DLS analysis was
224 conducted. According to Figure 2b, at 3 and 6 A, even after 6 h the degradation was not

complete and the MPs with the size of around 26 µm were observed. It can also be observed that no MPs with lower size was detected, which suggests the complete degradation of MPs at anode. At 9 A, however, after 2 h all the MPs are broken apparently into small particles. This result can be attributed to the degradation of MPs or decrease in their amount/size below the detectable values of the DLS analysis. Observation of a determinative effect of current intensity and time in EO process is in line with other studies (Dia et al., 2016; Drogui et al., 2007). To assess that, a DLS analysis was carried out with a concentration of 40 mg/L of MPs without treatment. That is almost the same amount of MP after its degradation at 9 A after 2 h. The results showed that the most frequent remained particle size was about 26 µm which confirms the remained MPs were not actually degraded into smaller particles.

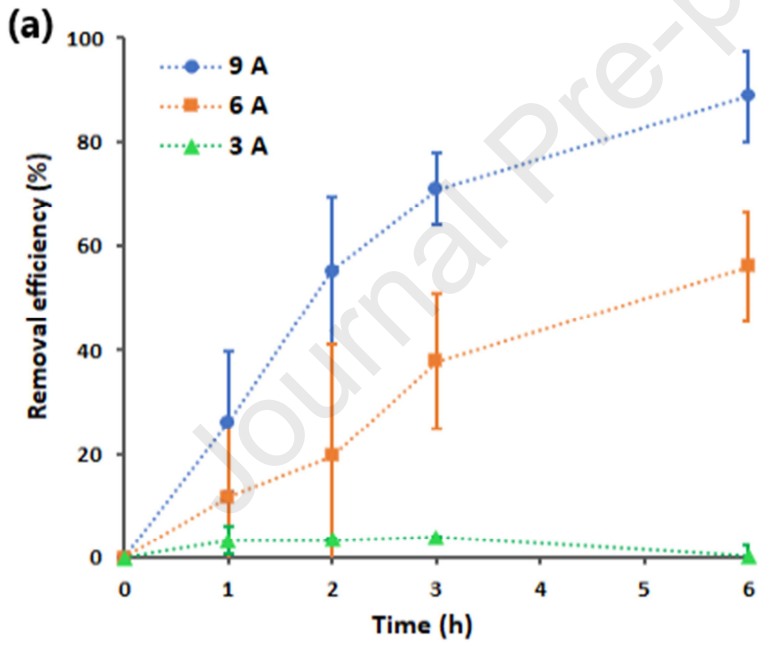

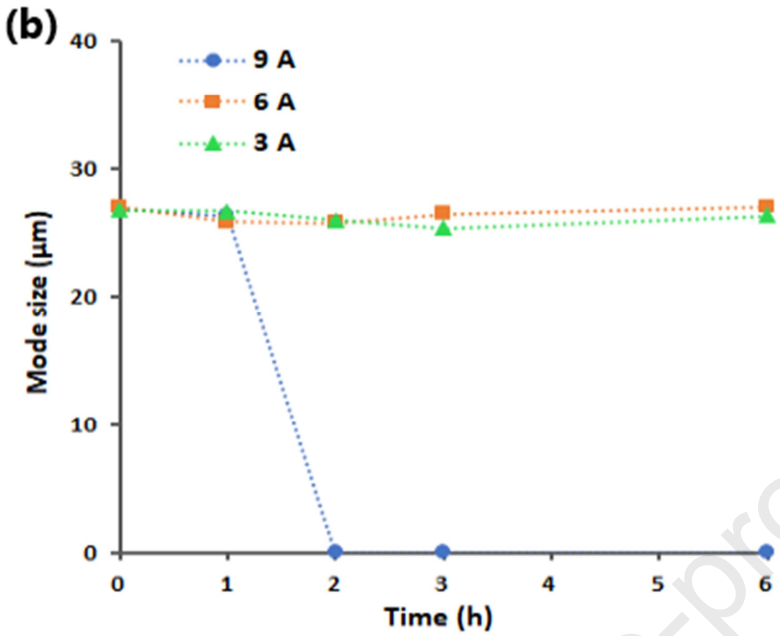


**Figure 2.** The effect of current density on the EO of MPs. (a) Removal efficiency (%), (b) Mode size (µm).

### 3.2.2. Effect of the anode surface area

The effect of anode surface area was evaluated by comparing the EO processes with 41.6 and 83 $cm^2$ surface areas at a constant of 9 A and 0.03 M $Na_2SO_4$ solution. As it can be seen from Figure 3a, in these conditions the anode surface area had almost no effect on the removal efficiency as after 6 h of operation the efficiency for both mentioned anodes reached around 90%. Despite this, at 41.6 and 83 $cm^2$ the potential was respectively 15 and 11 V, leading the reduction of energy consumption by increasing the anode surface area from 1080 to 792 $kWh/m^3$. The electrical resistivity decreased while increasing the electrode surface area. Figure 3b shows the effect of anode surface area on the reduction of the size of MPs. It shows that at higher anode surface area, no MPs with 26 µm size was detected by DLS analysis after 2 h. However, at smaller anode surface area, 6 h of electrooxidation time was required for MPs (with 26 µm size) disappearance in the solution. This discrepancy can be mainly attributed to the fact that when the anode area increases, the exchange surface area of electrode/electrolyte augments, so that shorter time was recorded for MPs degradation.

252

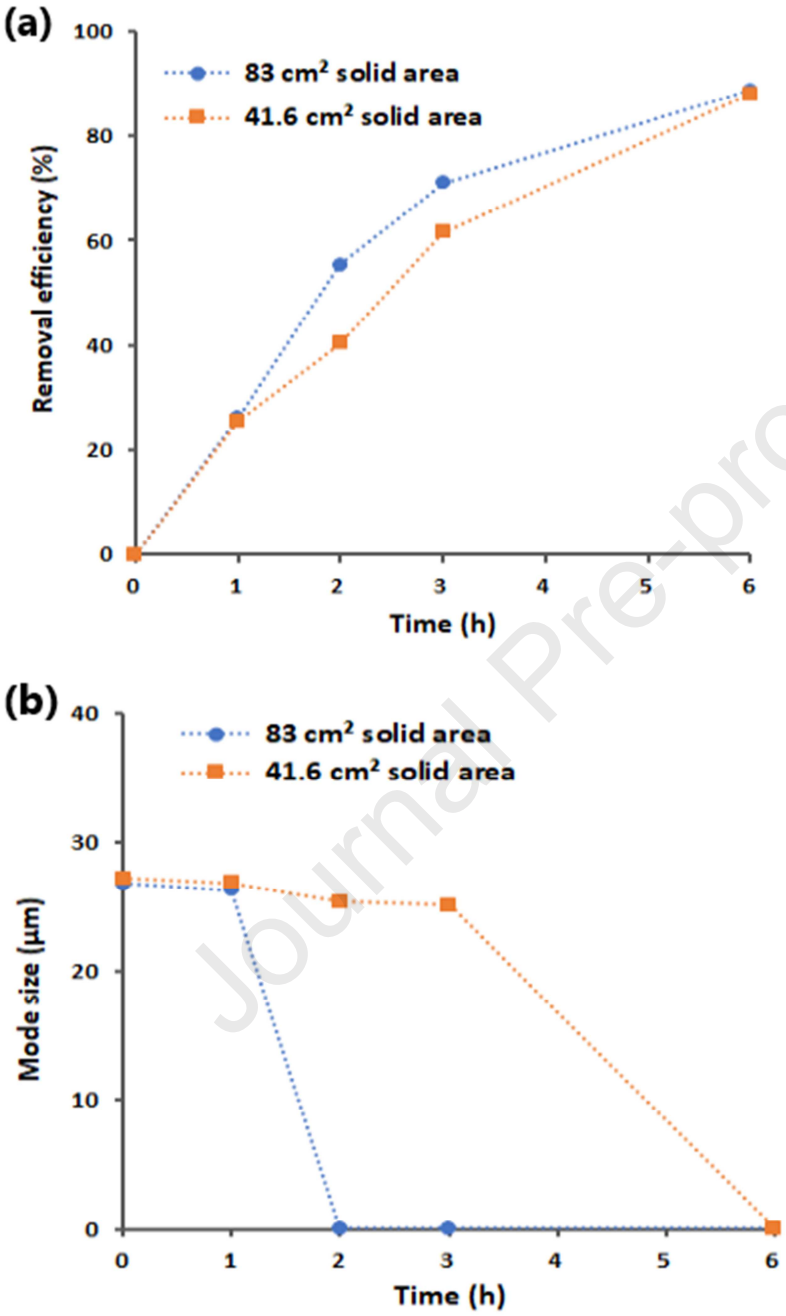


**Figure 3.** The effect of anode surface area on the EO of MPs. (a) Removal efficiency (%), (b) Mode size (µm).

253

254 **3.2.3. Effect of the anode material**

The electrode material defines the capacity for the generation of oxidants. As a result, the selection of electrode material is critical for an efficient EO process (Bhuta, 2014). The effect of anode material was analyzed by conducting experiments using BDD, MMO, and $IrO_2$ as anode material. For these experiments, the same intensity of 9 A and a $Na_2SO_4$ concentration of 0.03 M were applied during 6 h. Figure 4 shows the performance of EO process at different types of anode materials. A removal efficiency of 89%, 22%, and 12% was observed using BDD, $IrO_2$, and MMO, respectively (Figure 4a). It shows that BDD is substantially more powerful than $IrO_2$ and MMO for the degradation of MPs, as its reaction rate was around 4 and 7.4 times more than those two materials, respectively. Observation of a higher removal efficiency by BDD can be attributed to its higher rate of hydroxyl radical generation, as the previous research showed that BDD can produce around 4 times more hydroxyl radical than MMO (Yassine et al., 2018). According to Figure 4b, after 2 h of EO using BDD, no MPs was detected by DLS analysis. However, even after 6 h of EO using MMO and $IrO_2$, the MPs with initial size of 26 µm were detected. These results are in line with other researches that demonstrated that BDD has much higher oxidation potential than other common anodes such $IrO_2$ and MMO (Ciríaco et al., 2009; Flox et al., 2006; Martínez-Huitle et al., 2004; Zhao et al., 2009). BDD shows a great potential to react with pollutants due to the generation of a large amount of hydroxyl radicals (Frontistis et al., 2017; Yassine et al., 2018). However, for the case of MMO, it is shown that it has a strong reactivity with produced hydroxyls radicals which reduces the amount of available hydroxyls radicals (Durán et al., 2018; M. Panizza et al., 2001; Ozcan et al., 2008; Wang and Li, 2011).

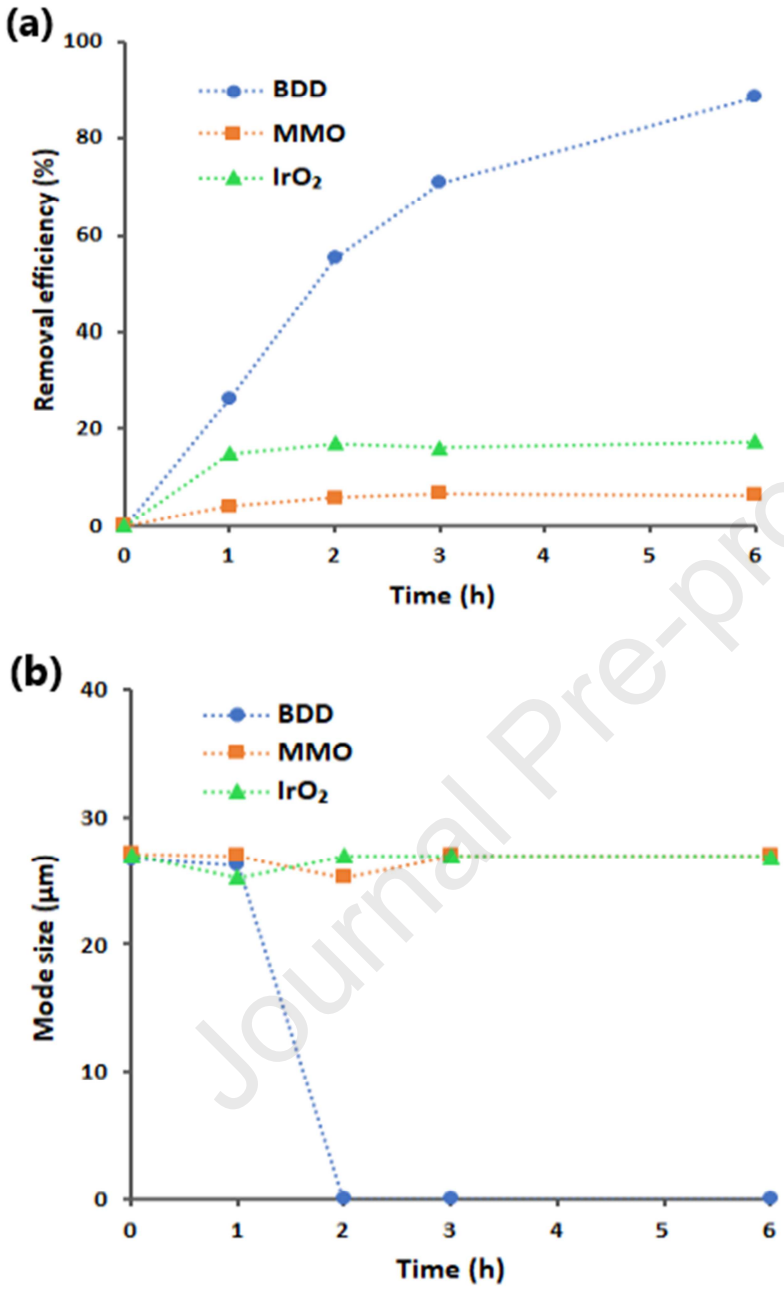


**Figure 4.** The effect of anode material on the EO of MPs. (a) Removal efficiency (%), (b) Mode size (µm).

277

278 **3.2.4. Effect of the supporting electrolyte type**

279 Some experiments were conducted using $Na_2SO_4$, $NaNO_3$, and NaCl as supporting
280 electrolyte to determine the effect of electrolyte type as well as the contribution of direct
281 and indirect oxidation of MPs. The electrolytes were used at different concentrations to

be able to impose the same current intensity of 9.0 A and electrical potential of around 14.9 V. The pH of solutions was fixed close to 6.0. Figure 5 presents the effect of electrolyte type on the removal efficiency and mode size of MPs. As Figure 5a shows, the removal efficiency was almost the same for NaCl and $Na_2SO_4$ till 2 h, but it increased faster afterwards using $Na_2SO_4$. For the case of $NaNO_3$, the removal efficiency was almost constant till 3 h and a significant increase was obtained between 3 and 6 h. As can be seen from Figure 5a, 89% removal efficiency was achieved after 6 h of EO using $Na_2SO_4$. However, 58% and 52% removal efficiencies were obtained with NaCl and $NaNO_3$, respectively. It shows that the rate of EO using $Na_2SO_4$ was 1.53 and 1.71 times higher than NaCl and $NaNO_3$, respectively. Other works also reported a higher EO rate using $Na_2SO_4$ which confirm the obtained result in this work (Durán et al., 2018; Panizza and Cerisola, 2005). According to Figure 5b, no MP with the initial size of around 26 µm was detected after 2 and 3 h using $Na_2SO_4$ and NaCl, respectively. However, even after 6 h, these MPs were detected using $NaNO_3$.

The different behavior of the electrolytes can be attributed to the action of different produced oxidizing species. In the case of NaCl, chloride ions are oxidized into chlorine gas ($Cl_2$) at anode (Eq. (4)), which reacts with water in the next step to form hypochlorous acid (Eq. (5)) and then dissociates into hypochlorite ions (Eq. (6)) (Durán et al., 2018; Ozcan et al., 2008). When $Na_2SO_4$ is used as supporting electrolyte, it dissociates into hydrogen sulfate and then persulfate ions ($S_2O_8^{2-}$) are formed through Eq. (7) (M. Panizza et al., 2001; Wang and Li, 2011). These highly reactive species could indirectly oxidize MPs and increase the removal efficiency. However, in the case of using $NaNO_3$ as supporting electrolyte, no oxidizing agent could be produced in the solution and only. It is worth noting that nitrate can be electrochemically reduced to ammonia (see Eqs. (8) and (9)) (Dia et al., 2017; Li et al., 2009; Renata and Luís, 2013).

$$2Cl^- \rightarrow Cl_2 + 2e^- \quad (4)$$

$$Cl_2 + H_2O \rightarrow HClO + Cl^- + H^+ \quad (5)$$

$$HClO \rightarrow ClO^- + H^+ \quad (6)$$

$$2HSO_4^- \rightarrow S_2O_8^{2-} + 2H^+ + 2e^- \quad (7)$$

$$NO_3^- + H_2O + 2e- \rightarrow NO_2^- + 2OH^- \quad (8)$$

$$NO_2^- + 5H_2O + 6e- \rightarrow NH_3 + 7OH^- \quad (9)$$

Accordingly, the relatively low percentage of MP removal recorded using $NaNO_3$ can be attributed to nitrate reduction into nitrite ($NO_2^-$) and ammonia ($NH_3$) (Dia et al., 2017). In fact, using $NaNO_3$ as supporting electrolyte, the electrochemical decomposition of MPs was only due to direct anodic oxidation (by means of $^{\bullet}OH$ radicals generated on the BDD). When $Na_2SO_4$ and NaCl were used as supporting electrolyte, the electrochemical decomposition of MPs could be carried out by using two paths: direct anodic oxidation and indirect electrochemical oxidation via mediators such as hypochlorous and persulfate ions. The direct anodic oxidation takes place on the surface of anode material, whereas indirect electrochemical oxidation takes place in aqueous solution. The two effects can lead to the formation of powerful oxidizing agents capable of effectively removing MPs.

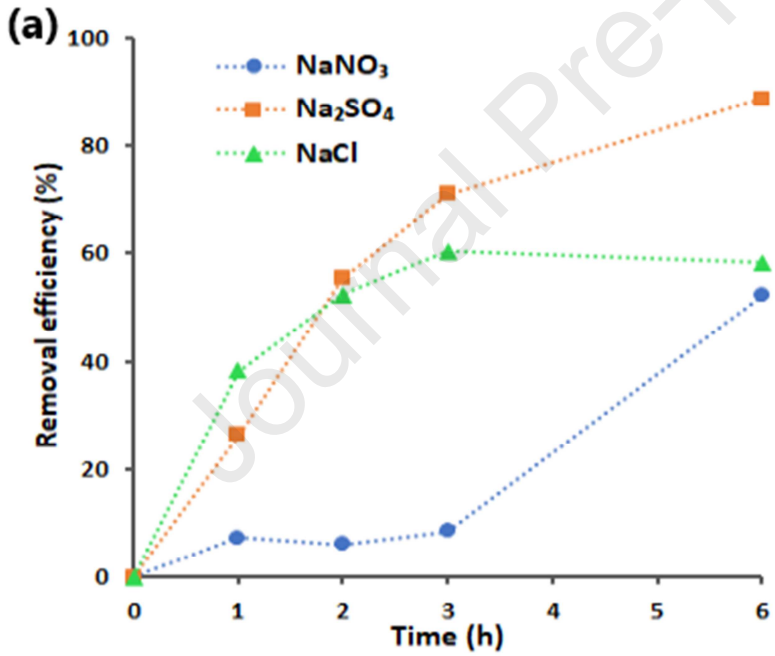

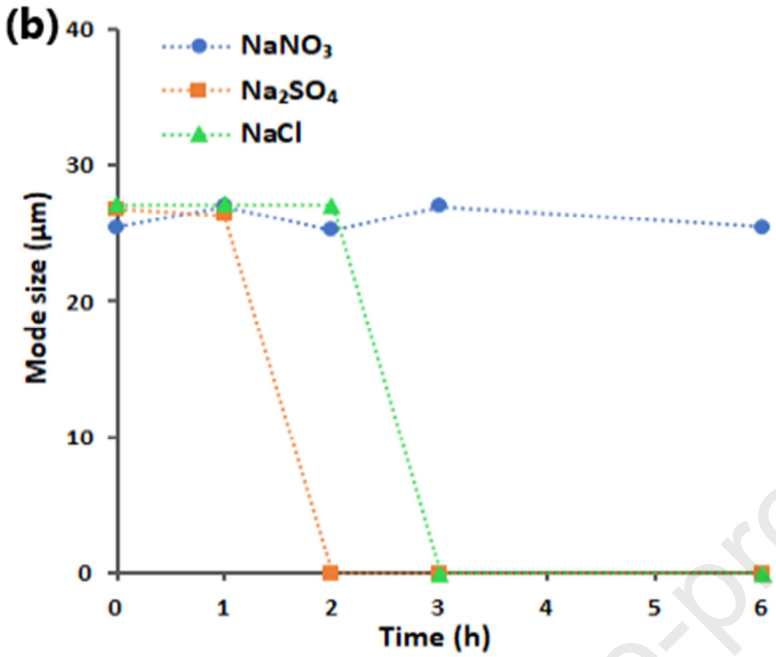


**Figure 5.** The effect of electrolyte type on the EO of MPs. (a) Removal efficiency (%), (b) Mode size (µm).

317

318 **3.2.5. Effect of the applied electrolyte concentration**

319 The electrolyte concentration is a determining parameter in the EO process as it affects
320 the operating costs in terms of electrolyte consumption and electrical energy
321 consumption. The influence of the electrolyte concentration on the removal efficiency
322 and mode size of MPs was investigated by conducting experiments at 0.03, 0.04, and
323 0.06 M $Na_2SO_4$. These experiments were conducted using one BDD anode at 9 A. As it
324 can be seen in Figure 6, the removal efficiency enhanced by increasing the electrolyte
325 concentration. MPs degradation of 25 ± 13%, 45 ± 17%, and 58 ± 21% were obtained
326 with electrolyte concentrations of 0.03, 0.04, and 0.06 M, respectively after 1 h of
327 electrooxidation. However, at prolonged time of 6 h, these removal efficiencies increased
328 to 89 ± 8%, 83 ± 8% and 84 ± 8% after 6 h of treatment which are almost the same. As it
329 can be seen from Figure 6b, no MPs with initial size of 26 µm was detected after 1 h at
330 0.06 M of electrolyte, however, this operating time increased to 2 h at 0.03 and 0.04 M.
331 Therefore, the DLS analysis confirmed that the rate of EO was higher at 0.06 M.

A cost analysis was performed to analyze the effect of electrolyte concentration on the operating cost of the EO process. The experimental results showed that, for electrolyte concentrations of 0.03, 0.04, and 0.06 M, the average electrical potential was around 15, 13, and 11 V, respectively. The electrical energy consumption analysis showed at 0.06 M, after 1 h (58 ± 21% removal efficiency) and 6 h (84 ± 8% removal efficiency) energy consumption were 132 and 1080 Kwh.m$^{-3}$, respectively.

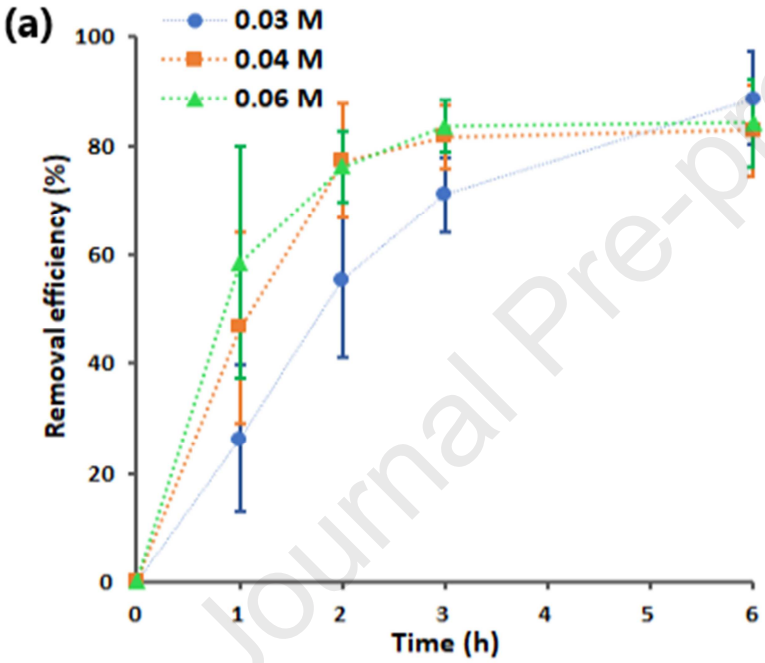

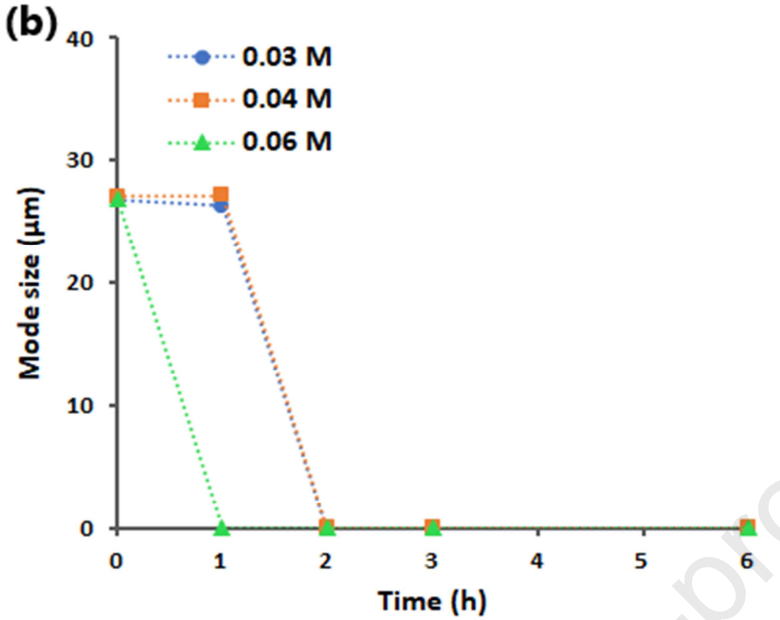


**Figure 6.** The effect of electrolyte concentration on the EO of MPs. (a) Removal efficiency (%), (b) Mode size (µm).

### 3.3. Total current efficiency analysis

The total current efficiency was calculated using Eq. (2) at 1, 2, 3, and 6 h for the experiments that were conducted using BDD anode material at 9 A with 0.06 M $Na_2SO_4$. The TCE values of 6%, 3%, 2%, and 1% were obtained after 1, 2, 3, and 6 h of EO, respectively. As expected, gradual decrease in TCE can be observed which demonstrates the loss of EO capacity by passing time (D. Gandini et al., 2000; Ignasi et al., 2008). This trend can be attributed to the decrease of the organic pollutants amount in the solution (Ciríaco et al., 2009; Sirés et al., 2006). On the other hand, as the rate of transfer of the MPs towards the electrode depends on its concentration, the mass transfer limitation increased by COD reduction through time. The low energy efficiency values obtained in this study could therefore be explained mainly by the nature of the aromatic polymer which resist against degradation and the mass transfer limits. Lower energy efficiency value than 10% with a TOC removal of nearly 90% was also reported for the EO of clofibric acid as an aromatic compound, using Ti/BDD with a current density of 150 $mA.cm^{-2}$ (Sirés et al., 2006).

### 3.4. Microscopic analysis of MPs before and after electrooxidation

SEM analysis was performed to find the change in the MPs size and shape during the EO process and evaluate the obtained results from weight loss and DLS analyses. The SEM image of MP particles before and after 1 h of EO are presented in Figure 7a and b, respectively. These figures clearly show the size of MPs is around 26 μm before and after electrooxidation, which confirm the obtained values in the mode size analysis. It is worth noting that no MPs were observed in the SEM analysis of the samples that were treated for more than 2 h of electrooxidation, confirming that MPs were completely degraded in these experimental conditions (according to results obtained from DLS analysis). The SEM images also showed the EO had no obvious effect on the spherical shape of the MPs. In Figure 7b, the formation of a layer of salt around the MP particles can be observed which is attributed to the deposition of electrolyte as layer of salt after drying the sample for the SEM analysis.

A statistical analysis was performed by ImageJ software on the obtained size of MPs using the SEM images. In these calculations, at least 20 data were collected to find an average value for the MPs diameter. This analysis showed the average size of MPs before and after 1 h electrooxidation time was 22.66 and 25.24 μm, respectively. This statistical analysis also confirmed the obtained average of MPs by DLS analysis.

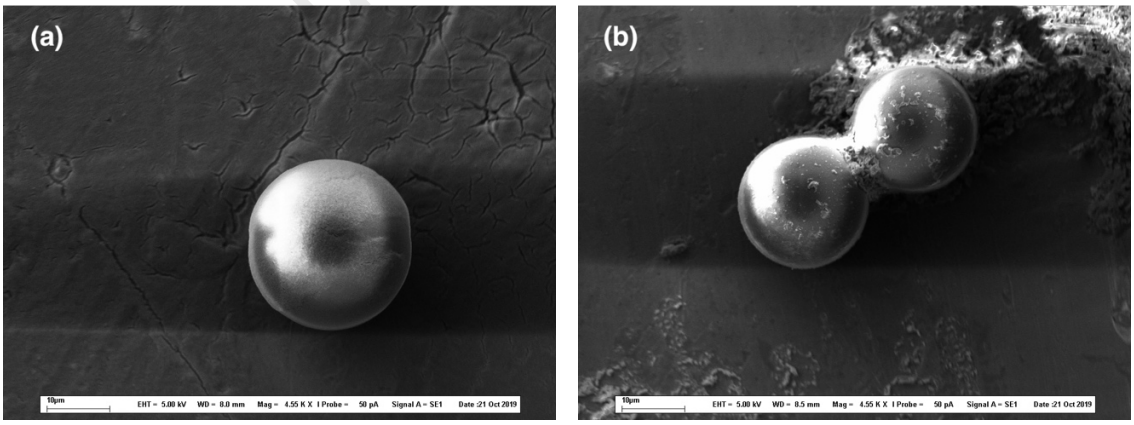


**Figure 7.** SEM images of MPs (a) before and (b) after 1 h of electrooxidation.

### 3.5. Spectroscopic analysis of MPs before and after electrooxidation

The MP samples were analyzed by FTIR spectroscopy to evaluate the formed functional groups on the surface of MPs. The FTIR spectra before and after electrooxidation are compared in Figure 8a. As it can be seen, in contrast to previous research on photo-oxidation (Cai et al., 2018), no peak at 1712 $cm^{-1}$ was recorded. This peak corresponds to C=O bonds. Accordingly, it may be concluded that the MPs were directly oxidized on the anode and no partially oxidized MPs were released into the water. This result may suggest that the direct oxidation of MPs on the surface of anode is the dominant mechanism in the degradation of MPs.

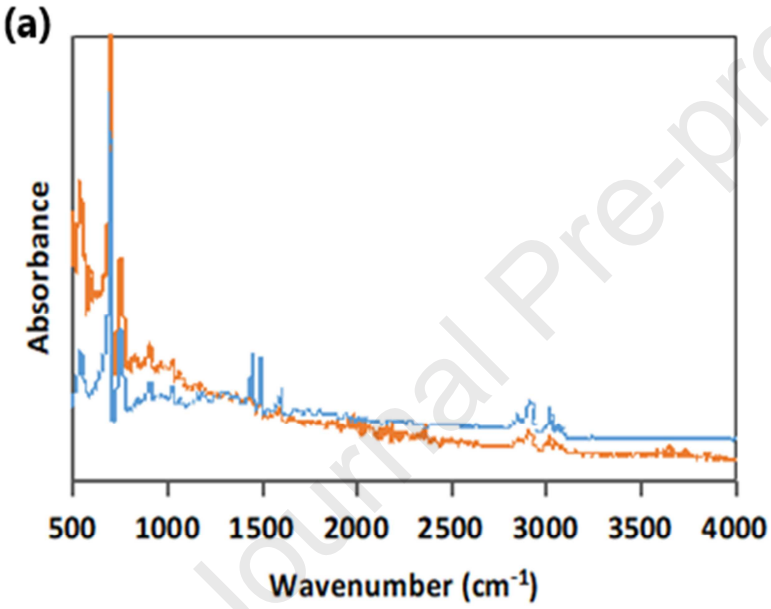

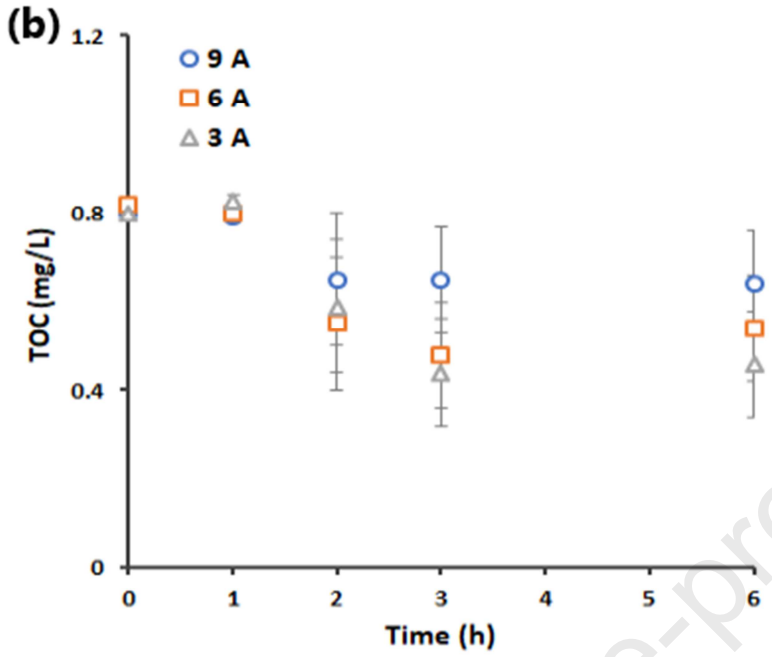


**Figure 8.** (a) FTIR spectra of MPs before (-) and after (-) 1 h of EO, (b) TOC analysis of filtered treated water at different current intensities.

### 3.6. TOC analysis of treated water

The treated water was filtered (0.22 µm filter pore size) and analyzed by TOC analyzer to evaluate the amount of generated liquid by-products through electrooxidation of MPs. To do so, the MPs were first filtered to separate the unreacted MPs from water and the filtrate was analyzed. The TOC analysis results for current intensities imposed of 3, 6, and 9 A are depicted in Figure 8b. Around 0.8 ± 0.02 mg/L of TOC was initially recorded before electrooxidation owing to the presence of surfactant in the filtered samples. As it can be seen, the TOC decreased through time for all current intensities that can be attributed to the degradation of surfactants in the purchased MP sample. According to Figure 8b, the TOC analysis showed no increase in the amount of organic carbon after electrooxidation time of 1, 2, 3, and 6 h. This result shows that no liquid by-product formed through electrooxidation of MP. This observation also shows no nanoplastics with a size lower than the filter pore size (0.22 µm) was available in the filtrate. Accordingly, all the MP particles were successfully filtered and calculated in the analysis of MP removal efficiency. The slight contradiction between the MPs mass removal

400 percentage results, and the mode size results in some samples can be related to
401 insufficient accuracy of DLS analysis at low MPs concentrations. It is worth underlining
402 that validity of the DLS analysis could be assured only when the transmission of light
403 was lower than 75-90 %, but the transmission passed this limit at removal percentages
404 higher than 40%.
405

406 **3.7. The proposed degradation mechanism**

407 The mechanism of polystyrene MPs degradation by anodic oxidation in water using BDD
408 electrode was proposed based on the obtained results in this study. At the first step,
409 hydroxyl radicals are generated from water on the surface of the anode as is shown in Eq.
410 (10). These radicals have a great affinity to make a reaction (Alves et al., 2013; Feng et
411 al., 2013; Urtiaga et al., 2014) and degrade polystyrene. As it can be seen from Eq. (11),
412 the generated hydroxyl radicals initiate the degradation of polystyrene with breaking
413 carbon-hydrogen bond which leads the formation of carbon-oxygen bond. In the next
414 step, the polymeric bond can be broken through breakage of C-C or C-Ph bonds (where
415 Ph denotes phenolic group, see Eq. (12)). The short lifetime and the high reactivity of the
416 hydroxyl radicals makes the carbonyl bond detection very difficult (García-Gómez et al.,
417 2014). Further oxidation of the degraded polymeric chain can lead to additional
418 decomposition of the formed compounds and finally complete oxidation to produce
419 carbon dioxide and water, based on Eq. (13), as is reported by previous researchers (E.
420 Weiss et al., 2006; Marco and Giacomo, 2009; Sirés et al., 2006). A more detailed
421 mechanism of EO of MP is currently under investigation in our research group.

$$BDD + H_2O \rightarrow BDD(OH^{\circ}) + H^+ + e^- \quad (10)$$

$$-(CH_2 - CHPh - CH_2 -) + BDD(OH^{\circ}) \rightarrow -(CH_2 - CO^{\circ}Ph - CH_2 -) + H^+ + e^- + BDD \quad (11)$$

$$-(CH_2 - CO^{\circ}Ph - CH_2 -) \rightarrow CH_2 - CO - Ph + -CH_2^{\circ} \quad (12)$$

Or $-(CH_2 - CO^{\circ}Ph - CH_2 -) \rightarrow CH_2 - CO - CH_2 + Ph^{\circ}$

$$CH_2 - CO - Ph; -CH_2^{\circ}; CH_2 - CO - CH_2; Ph^{\circ}; + BDD(OH^{\circ}) \rightarrow CO_2 + H_2 \quad (13)$$

422

423 **3.8. Cost analysis**

A cost analysis was performed at optimum condition to analyze the effect of electrolyte type on the operating cost of the current EO process. The cost analysis data are presented in Table 1. As it can be seen, the energy consumption (calculated using Eq. (3)) of $Na_2SO_4$ electrolyte was higher than $NaNO_3$ and NaCl, which was attributed to higher applied electrical potential at constant electrical current intensity during this process. In addition, it can be seen that energy cost was dominant in the value of total operating cost. After 6 h EO, the total operating cost was 68.5, 59.9, and 57.6 \$/$m^3$ for $Na_2SO_4$, NaCl, and $NaNO_3$, respectively, during which 89%, 58%, and 52% removal efficiencies were obtained. After 1 h EO, which 23%, 38%, and 7% removal efficiencies were obtained, these values were 11.4, 8.9, and 10.4 \$/$m^3$, respectively. These results are comparable with the literature results of energy consumption analysis for recalcitrant pollutants by EO (Canizares et al., 2006; Durán et al., 2018). It can be concluded from this comparison that the treatment of MPs using $Na_2SO_4$ for 6 h is the best condition because a significantly higher removal efficiency was obtained without any substantial increase in the total operating cost. Moreover, in contrast to NaCl, the EO process using $Na_2SO_4$ does not produce toxic chlorine gas. (Perren et al., 2018) reported the cost of MPs separation with electrocoagulation process to be around £0.05 (Can\$ 0.086). The lower cost than the current work is attributed to the big size of MPs (around 0.3 mm) as well as the separative nature of process that does not degrade the MPs. It is worth mentioning that research is being conducted on hybrid advanced oxidation processes to economically treat complex water matrix containing MPs like laundry wastewater. Accordingly, the EO could be a feasible process for the degradation of MPs in waters, but further research is required to elucidate the influences of anode fouling and mutual contaminants interactions.

**Table 1.** Cost analysis of MP EO using $Na_2SO_4$, $NaNO_3$, and NaCl as electrolyte after 1 and 6 h.

| | **Unit** | **Electrolyte type** | | |
|---|---|---|---|---|
| | | **$Na_2SO_4$** | **NaCl** | **$NaNO_3$** |
| **Removal efficiency (%)** | (%/6 h) | 89 | 58 | 52 |
| | (%/h) | 23 | 38 | 7 |
| **Energy consumption** | (kWh/$m^3$/6 h) | 1120 | 995 | 932 |

| | | | | |
|---|---|---|---|---|
| | ($kWh/m^3/h$) | 169 | 145 | 146 |
| **Energy cost** | ($/6 h) | 67.2 | 59.7 | 55.9 |
| | ($/h) | 10.1 | 8.7 | 8.7 |
| **Electrolyte cost** | ($) | 1.3 | 0.2 | 1.7 |
| **Total operating cost** | ($/6 $h/m^3$) | 68.5 | 59.9 | 57.6 |
| | ($/$h/m^3$) | 11.4 | 8.9 | 10.4 |

## Conclusion

The EO process using BDD anode electrode is a feasible technology for the treatment of water contaminated by MPs. Using $Na_2SO_4$ (0.03 M) as supporting electrolyte and a current intensity of 9 A during 6 h of electrolysis time ensures a high degradation efficiently of MPs (89 ± 8 %). The DLS results suggested that the MPs did not break into the smaller particles and they transformed directly into the gaseous products (such as $CO_2$). The SEM, TOC, and FTIR analyses also confirmed the mineralization of MPs during the application of EO process, by indicating no broken MPs, detecting no organic carbon, and observing no oxidized functional group after MPs oxidation. The EO process could be the basis of a process for MPs degradation in real wastewaters, but the consequences of anode fouling and mutual contaminants interactions must be further investigated.

## Acknowledgements

The authors would like to acknowledge the financial support from the Fonds de recherche du Québec – Nature et technologies (FRQNT), the CREATE-TEDGIEER program, National Sciences and Engineering Research Council of Canada (NSERC), and Canadian Francophonie Scholarship Program.

## References

Alves, S.A., Ferreira, T.C.R., Migliorini, F.L., Baldan, M.R., Ferreira, N.G., Lanza, M.R.V., 2013. Electrochemical degradation of the insecticide methyl parathion using a boron-doped diamond film anode. J Electroanal Chem 702, 1-7.

Besseling, E., Wang, B., Lurling, M., Koelmans, A.A., 2014. Nanoplastic affects growth of S. obliquus and reproduction of D. magna. Environ Sci Technol 48, 12336-12343.

Bhuta, H., 2014. Advanced treatment technology and strategy for water and wastewater management. Industrial Wastewater Treatment, Recycling and Reuse, 1st ed; Ranade, VV, Bhandari, VM, Eds, 193-213.

Bouwmeester, H., Hollman, P.C., Peters, R.J., 2015. Potential Health Impact of Environmentally Released Micro and Nanoplastics in the Human Food Production Chain : Experiences from Nanotoxicology. Environ Sci Technol 49, 8932-8947.

Cai, L., Wang, J., Peng, J., Wu, Z., Tan, X., 2018. Observation of the degradation of three types of plastic pellets exposed to UV irradiation in three different environments. Sci Total Environ 628, 740-747.

Canizares, P., A. Gadri, J.L., Lobato, J., Lobato, J., Nasr, B., Paz, R., Rodrigo, M.A., Sae, C., 2006. Electrochemical Oxidation of Azoic Dyes with Conductive-Diamond Anodes. Ind Eng Chem Res 45, 3468-3473.

Chae, Y., An, Y.J., 2017. Effects of micro- and nanoplastics on aquatic ecosystems: Current research trends and perspectives. Mar Pollut Bull 124, 624-632.

Ciríaco, L., Anjo, C., Correia, J., Pacheco, M.J., Lopes, A., 2009. Electrochemical degradation of Ibuprofen on Ti/Pt/$PbO_2$ and Si/BDD electrodes. Electrochim Acta 54, 1464-1472.

Cole, M., Lindeque, P., Halsband, C., Galloway, T.S., 2011. Microplastics as contaminants in the marine environment: a review. Mar Pollut Bull 62, 2588-2597.

D. Gandini, E. Mahe, P.A. Michaud, W. Haenni, A. Perret, Comninellis, C., 2000. Oxidation of carboxylic acids at boron-doped diamond electrodes for wastewater treatment. J Appl Electrochem 30, 1345-1350.

Dia, O., Drogui, P., Buelna, G., Dubé, R., 2017. Strategical approach to prevent ammonia formation during electrocoagulation of landfill leachate obtained from a biofiltration process. Separation and Purification Technology 189, 253-259.

Dia, O., Drogui, P., Dubé, R., Buelna, G., 2016. Utilisation des procédés électrochimiques et leurs combinaisons avec les procédés biologiques pour le traitement des lixiviats de sites d'enfouissement sanitaires-revue de littérature. Journal of Water Science 29, 63-89.

Drogui, P., Blais, J.-F., Mercier, G., 2007. Review of electrochemical technologies for environnement applications. Recent Pat. Eng. 1, 257-272.

Durán, F.E., de Araújo, D.M., do Nascimento Brito, C., Santos, E.V., Ganiyu, S.O., Martínez-Huitle, C.A., 2018. Electrochemical technology for the treatment of real washing machine effluent at pre-pilot plant scale by using active and non-active anodes. J Electroanal Chem 818, 216-222.

E. Weiss, K. Groenen-Serrano, Savall, A., 2006. Electrochemical Degradation of Sodium Dodecylbenzene Sulfonate on Boron Doped Diamond and Lead Dioxide Anode. J New Mater Electrochem Syst 9, 249-256.

Enfrin, M., Dumee, L.F., Lee, J., 2019. Nano/microplastics in water and wastewater treatment processes - Origin, impact and potential solutions. Water Res 161, 621-638.

Feng, L., van Hullebusch, E.D., Rodrigo, M.A., Esposito, G., Oturan, M.A., 2013. Removal of residual anti-inflammatory and analgesic pharmaceuticals from aqueous systems by electrochemical advanced oxidation processes. A review. Chem Eng J 228, 944-964.

Flox, C., Cabot, P.L., Centellas, F., Garrido, J.A., Rodriguez, R.M., Arias, C., Brillas, E., 2006. Electrochemical combustion of herbicide mecoprop in aqueous medium using a flow reactor with a boron-doped diamond anode. Chemosphere 64, 892-902.

519 Francisca, C.M., Sergi, G.-S., Vítor, J.P.V., Rui, A.R.B., Enric, B., 2013. Decolorization and
520 mineralization of Sunset Yellow FCF azo dye by anodic oxidation, electro-Fenton, UVA
521 photoelectro-Fenton and solar photoelectro-Fenton processes. Appl Catal B: Environ 142, 877-
522 890.
523 Frontistis, Z., Antonopoulou, M., Venieri, D., Konstantinou, I., Mantzavinos, D., 2017. Boron-
524 doped diamond oxidation of amoxicillin pharmaceutical formulation: Statistical evaluation of
525 operating parameters, reaction pathways and antibacterial activity. J Environ Manage 195, 100-
526 109.
527 Ganiyu, S.O., Oturan, N., Raffy, S., Esposito, G., van Hullebusch, E.D., Cretin, M., Oturan, M.A.,
528 2017. Use of Sub-stoichiometric Titanium Oxide as a Ceramic Electrode in Anodic Oxidation and
529 Electro-Fenton Degradation of the Beta-blocker Propranolol: Degradation Kinetics and
530 Mineralization Pathway. Electrochim Acta 242, 344-354.
531 García-Gómez, C., Drogui, P., Zaviska, F., Seyhi, B., Gortáres-Moroyoqui, P., Buelna, G., Neira-
532 Sáenz, C., Estrada-alvarado, M., Ulloa-Mercado, R.G., 2014. Experimental design methodology
533 applied to electrochemical oxidation of carbamazepine using Ti/$PbO_2$ and Ti/BDD electrodes. J
534 Electroanal Chem 732, 1-10.
535 Garcia-Segura, S., Keller, J., Brillas, E., Radjenovic, J., 2015. Removal of organic contaminants
536 from secondary effluent by anodic oxidation with a boron-doped diamond anode as tertiary
537 treatment. J Hazard Mater 283, 551-557.
538 Gigault, J., Halle, A.T., Baudrimont, M., Pascal, P.Y., Gauffre, F., Phi, T.L., El Hadri, H., Grassl, B.,
539 Reynaud, S., 2018. Current opinion: What is a nanoplastic? Environ Pollut 235, 1030-1034.
540 Hidalgo-Ruz, V., Gutow, L., Thompson, R.C., Thiel, M., 2012. Microplastics in the marine
541 environment: a review of the methods used for identification and quantification. Environ Sci
542 Technol 46, 3060-3075.
543 Ignasi, S., Enric, B., Giacomo, C., Marco, P., 2008. Comparative depollution of mecoprop aqueous
544 solutions by electrochemical incineration using BDD and $PbO_2$ as high oxidation power anodes.
545 J Electroanal Chem 613, 151–159.
546 Jeong, C.B., Won, E.J., Kang, H.M., Lee, M.C., Hwang, D.S., Hwang, U.K., Zhou, B., Souissi, S., Lee,
547 S.J., Lee, J.S., 2016. Microplastic Size-Dependent Toxicity, Oxidative Stress Induction, and p-JNK
548 and p-p38 Activation in the Monogonont Rotifer (Brachionus koreanus). Environ Sci Technol 50,
549 8849-8857.
550 Lambert, S., Wagner, M., 2016. Characterisation of nanoplastics during the degradation of
551 polystyrene. Chemosphere 145, 265-268.
552 Lares, M., Ncibi, M.C., Sillanpaa, M., Sillanpaa, M., 2018. Occurrence, identification and removal
553 of microplastic particles and fibers in conventional activated sludge process and advanced MBR
554 technology. Water Res 133, 236-246.
555 Lee, K.W., Shim, W.J., Kwon, O.Y., Kang, J.H., 2013. Size-dependent effects of micro polystyrene
556 particles in the marine copepod Tigriopus japonicus. Environ Sci Technol 47, 11278-11283.
557 Li, L., Xu, G., Yu, H., Xing, J., 2018. Dynamic membrane for micro-particle removal in wastewater
558 treatment: Performance and influencing factors. Sci Total Environ 627, 332-340.
559 Li, M., Feng, C., Zhang, Z., Lei, X., Chen, R., Yang, Y., Sugiura, N., 2009. Simultaneous reduction of
560 nitrate and oxidation of by-products using electrochemical method. J Hazard Mater 171, 724-
561 730.
562 M. Panizza , P.A. Michaud , G. Cerisola, Ch. Comninellis b, 2001. Anodic oxidation of 2-naphthol
563 at boron-doped diamond electrodes. J Electroanal Chem 507, 206–214.
564 Marco, P., Giacomo, C., 2009. Direct And Mediated Anodic Oxidation of Organic Pollutants.
565 Chem Rev 109, 6541–6569.

566 Martínez-Huitle, C.A., Quiroz, M.A., Comninellis, C., Ferro, S., Battisti, A.D., 2004.
567 Electrochemical incineration of chloranilic acid using Ti/$IrO_2$, Pb/$PbO_2$ and Si/BDD electrodes.
568 Electrochim Acta 50, 949-956.
569 Moore, C.J., 2008. Synthetic polymers in the marine environment: a rapidly increasing, long-
570 term threat. Environ Res 108, 131-139.
571 Ozcan, A., Sahin, Y., Koparal, A.S., Oturan, M.A., 2008. Propham mineralization in aqueous
572 medium by anodic oxidation using boron-doped diamond anode: influence of experimental
573 parameters on degradation kinetics and mineralization efficiency. Water Res 42, 2889-2898.
574 Panizza, M., Cerisola, G., 2005. Application of diamond electrodes to electrochemical processes.
575 Electrochim Acta 51, 191-199.
576 Perren, W., Wojtasik, A., Cai, Q., 2018. Removal of Microbeads from Wastewater Using
577 Electrocoagulation. ACS Omega 3, 3357-3364.
578 Phonsy, P.D., Anju, S.G., Jyothi, K.P., Yesodharan, S., Yesodharan, E.P., 2015. Semiconductor
579 mediated photocatalytic degradation of plastics and recalcitrant organic pollutants in water:
580 effect of additives and fate of insitu formed $H_2O_2$. J Adv Oxid Technol 18, 85-97.
581 Plastics Europe. Plastics-The Facts., 2019. An analysis of European plastics production, demand
582 and waste data.
583 Renata, B.A.d.S., Luís, A.M.R., 2013. Phenol Electrooxidation in Different Supporting Electrolytes
584 Using Boron-Doped Diamond Anodes. Int J Electrochem Sci 8, 643 - 657.
585 Rossi, G., Barnoud, J., Monticelli, L., 2014. Polystyrene Nanoparticles Perturb Lipid Membranes. J
586 Phys Chem Lett 5, 241-246.
587 Satoshi, H., Nick, S., Yoshiharu, H., Hidaka, H., 1998. Photocatalyzed Degradation of Polymers in
588 Aqueous Semiconductor Suspensions. 3. Photooxidation of a Solid Polymer: $TiO_2$-Blended
589 Poly(vinyl chloride) Film. Environ Sci Technol 32, 4010-4016.
590 Sirés, I., Cabot, P.L., Centellas, F., Garrido, J.A., Rodríguez, R.M., Arias, C., Brillas, E., 2006.
591 Electrochemical degradation of clofibric acid in water by anodic oxidation. Electrochim Acta 52,
592 75-85.
593 Souza, F.L., Lanza, M.R., Llanos, J., Saez, C., Rodrigo, M.A., Canizares, P., 2015. A wind-powered
594 BDD electrochemical oxidation process for the removal of herbicides. J Environ Manage 158, 36-
595 39.
596 Sun, J., Dai, X., Wang, Q., van Loosdrecht, M.C.M., Ni, B.J., 2019. Microplastics in wastewater
597 treatment plants: Detection, occurrence and removal. Water Res 152, 21-37.
598 Talvitie, J., Mikola, A., Koistinen, A., Setala, O., 2017. Solutions to microplastic pollution -
599 Removal of microplastics from wastewater effluent with advanced wastewater treatment
600 technologies. Water Res 123, 401-407.
601 Urtiaga, A., Fernandez-Castro, P., Gómez, P., Ortiz, I., 2014. Remediation of wastewaters
602 containing tetrahydrofuran. Study of the electrochemical mineralization on BDD electrodes.
603 Chem Eng J 239, 341-350.
604 Wang, J.-g., Li, X.-m., 2012. Electrochemical treatment of wastewater containing chlorophenols
605 using boron-doped diamond film electrodes. J Cent South Univ 19, 1946-1952.
606 Wegner, A., Besseling, E., Foekema, E.M., Kamermans, P., Koelmans, A.A., 2012. Effects of
607 nanopolystyrene on the feeding behavior of the blue mussel (Mytilus edulis L.). Environ Toxicol
608 Chem 31, 2490-2497.
609 Yassine, O., Bhagyashree, T., Antonin, A., Marc-Antoine, V., Sokhna, D., Ndiaye,, Patrick, D.,
610 Rajeshwhar, D., Tyagi, , Sebastien, S., Melanie, D., Gerardo, B., Rino, D., 2018. Synthetic hospital
611 wastewater treatment by coupling submerged membrane bioreactor and electrochemical
612 advanced oxidation process: Kinetic study and toxicity assessment. Chemosphere 193, 160-169.

613 Zarfl, C., Matthies, M., 2010. Are marine plastic particles transport vectors for organic pollutants
614 to the Arctic? Mar Pollut Bull 60, 1810-1814.
615 Zhao, X., Hou, Y., Liu, H., Qiang, Z., Qu, J., 2009. Electro-oxidation of diclofenac at boron doped
616 diamond: Kinetics and mechanism. Electrochim Acta 54, 4172-4179.
617 Zhuo, Q., Luo, M., Guo, Q., Yu, G., Deng, S., Xu, Z., Yang, B., Liang, X., 2016. Electrochemical
618 Oxidation of Environmentally Persistent Perfluorooctane Sulfonate by a Novel Lead Dioxide
619 Anode. Electrochim Acta 213, 358-367.
620 Ziajahromi, S., Neale, P.A., Rintoul, L., Leusch, F.D., 2017. Wastewater treatment plants as a
621 pathway for microplastics: Development of a new approach to sample wastewater-based
622 microplastics. Water Res 112, 93-99.

623

- Degradation of MPs by EO process using catalytic anode materials was investigated.
- Synthetic suspension was prepared using polystyrene microbeads with 26 µm size.
- Current intensity, type of anode and electrolyte greatly affected MPs degradation.
- Performance of EO process was evaluated using DLS, SEM, TOC and FTIR analyses.
- EO process can degrade more than 58 ± 21% of MPs in 1 h of electrolysis.

**Declaration of interests**

☐ The authors declare that they have no known competing financial interests or personal relationships that could have appeared to influence the work reported in this paper.

☒The authors declare the following financial interests/personal relationships which may be considered as potential competing interests:

Fonds de recherche du Québec – Nature et technologies (FRQNT)
CREATE-TEDGIEER program
National Sciences and Engineering Research Council of Canada (NSERC)
Canadian Francophonie Scholarship Program